

# Renewable diesel blends production from hydrothermal liquefaction of food waste: A novel approach coupling fractional distillation and emulsification



Zixin Wang <sup>a</sup>, Buchun Si <sup>a,b,\*</sup>, Sabrina Summers <sup>a</sup>, Yuanhui Zhang <sup>a,\*</sup>

<sup>a</sup> Department of Agricultural and Biological Engineering, University of Illinois at Urbana-Champaign, IL 61801, USA

<sup>b</sup> Key Laboratory of Agricultural Engineering in Structure and Environment, Ministry of Agriculture and Rural Affairs, College of Water Resources and Civil Engineering, China Agricultural University, Beijing, 100083, China

## ARTICLE INFO

### Keywords:

Hydrothermal liquefaction  
Food waste  
Fractional distillation  
Emulsification  
Renewable diesel blends

## ABSTRACT

Hydrothermal liquefaction (HTL) is a promising approach for producing biocrude oil from wet biowaste, but the suboptimal properties of HTL biocrude hinder its direct utilization as transportation fuel. This study presents an innovative approach by integrating fractional distillation and emulsification to upgrade HTL biocrude derived from food waste into renewable diesel blends. Fractional distillation is effective in removing metals, heavy fractions, and impurities, thus improving the physicochemical properties of the biocrude. Subsequent emulsification of distillates (10–30 wt%) with diesel, using Atlox 4912 as the surfactant, ensures a homogeneous mixture. The solubility of biocrude in diesel increased from 34.80 wt% to 100 wt% after distillation. Compared to direct HTL biocrude emulsification, distillate emulsion exhibited a 17.22% and 20.89% reduction in oxygen and nitrogen content, respectively, as well as significant improvements in terms of higher heating value, carbon and energy recoveries, and reduction of metal elements. The resulting emulsion demonstrated comparable viscosity, molecular weight, and boiling point distributions to the commercial diesel. Moreover, the oxidation and thermal stability tests revealed superior performance of distillate emulsion, with no observable sedimentation during the storage period. In contrast, direct biocrude emulsion experienced 14.37 wt% of phase separation. The mechanism of emulsion aging was then investigated, providing the basis for obtaining emulsions with preferable yield and quality. The comparative evaluation in this study showed that the integrated approach of fractional distillation and emulsification enhances the feasibility and quality of producing renewable diesel blends from HTL biocrude.

## 1. Introduction

Food waste has increasingly been recognized as a significant social, economic, and environmental issue. Its disposal in landfills and subsequent decomposition generate gases that contribute to the greenhouse effect, and leachate that contaminates the surrounding soil and water resources [1,2]. To address this problem, hydrothermal liquefaction (HTL) has emerged as a promising approach for converting food waste into biocrude oil, offering a sustainable solution for waste management and energy production [3]. Food waste is produced at every stage of the food supply chain and includes various categories with distinct chemical compositions. Proteins are mostly found in meat and fish processing wastes; lignin exists mainly in vegetable and fruit wastes; and lipids are primarily present in meat, seed, and some fruit processing residues,

which significantly contribute to biocrude production [4]. The composition and interactions of these different compounds can directly affect the quantity and quality of the biocrude. Therefore, previous studies have explored the HTL of food waste with different biochemical compositions using model compounds and representative real food wastes [5,6]; as well as the co-liquefaction of food waste with other types of waste (such as plastics, wood sawdust, and algae [7,8]) to control the biocrude properties, and make full use of the feedstock. Additionally, the impact of process parameters on HTL has been widely studied, including the heating rate [9], kinetic severity factor (which relates to temperature and time), solid content, and other critical factors [10].

The HTL biocrude oils can be used for power generation, but their intrinsic limitations, such as high viscosity, low heating value, and poor

\* Corresponding authors.

E-mail addresses: [sibuchun@cau.edu.cn](mailto:sibuchun@cau.edu.cn) (B. Si), [yzhang1@illinois.edu](mailto:yzhang1@illinois.edu) (Y. Zhang).

thermal stability, impede their direct utilization as transportation fuels [11]. Various technologies have been investigated for upgrading biocrude, such as hydrotreating, hydrocracking, solvent extraction, esterification, and steam reforming. However, these techniques typically involve complex equipment, expensive catalysts and solvents, high energy input, and often result in fuels with suboptimal quality [12,13]. From a technical and economic aspect, another strategy, emulsification, has been developed to upgrade biocrude by combining it with a base fuel such as diesel [14–16].

Emulsification offers several advantages: it is a simple process that does not require complex chemical reactions; can be carried out under mild conditions; and is effective in improving fuel properties and helps to maximize the utilization of biocrude oil. External energy, often in the form of stirring or heating, is typically involved to facilitate the emulsification, because of the need to overcome kinetic energy barriers and mass transfer limitations that impede spontaneous formation of emulsions [17]. Emulsification can be driven by a variety of mechanisms, such as generating kinetic energy through mechanical agitation and high-speed dispersion machines followed by colloid mills and homogenizers; in addition, ultrasonic emulsification driven by acoustic energy and membrane emulsification driven by transmembrane pressure have been explored, each offering distinct advantages in terms of product quality and energy input [13]. Particularly, ultrasonification is good at emulsifying heavy oil compounds, due to its high frequency sound waves create a homogeneous emulsion of small droplets with long-term stability [18]. The addition of a surfactant or emulsifier is also a crucial step in blending the immiscible streams of biocrude with base fuel. Within an emulsion, the dispersed or droplet phase (biocrude) is enveloped by a layer of the continuous phase (base fuel). The surfactant creates a thin interfacial film between the two liquids and effectively minimizing the contact, coalescence, and aggregation of the dispersed phase [19,20].

Results from previous emulsification studies of food waste biocrude have shown that emulsions possess improved fuel properties, including higher heating value, and reduced viscosity and acidity [18,21–23]. However, challenges persist, such as limited efficiency and miscibility issues, resulting in only part of the biocrude oil dissolving into the base fuel and remaining stable [24]. The solubility of food waste biocrude in diesel was reported to be 18.74–75.67 wt% at biocrude fractions of 10–30 wt%, with the aid of surfactant Atlox 4912 [18]. Higher biocrude solubility was achieved with the use of a co-surfactant [21]. Biocrude oil is a complex mixture of multiple compounds with varying solubility in the base fuels, making it challenging to achieve optimal distribution in emulsion systems, particularly between polar and non-polar phases. Guo et al. found that the heavy fractions of biocrude have difficulty forming stable emulsions, the large droplet sizes making them stable for only a few minutes, whereas light and middle fractions exhibit greater stability of up to a month [25]. Therefore, pretreatment of biocrude becomes crucial to enhance emulsification efficacy.

Fractional distillation has been proved to be a promising technology for pretreating crude oil, which is primarily a physical separation process without the addition of catalysts [26–28]. It can effectively remove the heavier fractions and impurities from the oil, decrease the oxygen and nitrogen content, lower the polarity of crude oil, and result in the production of distillates with better physicochemical properties and easier to be blended with base fuels [29–31]. Compared to crude oil, distillates demonstrate enhanced stability, mitigating the potential changes in elemental composition, viscosity, acidity, and molecular weight during storage, a common concern with crude oil due to the presence of heteroatoms and unsaturated bonds [32]. The instability of biocrude can lead to the formation of insoluble sediments, making the fuel unreliable and unusable. In comparison, the properties of the distillate were not significantly affected during 16 weeks of storage, indicating its superior stability [32]. These distinct advantages make fractional distillation an ideal candidate for combination with emulsification to upgrade crude oil for fuel production. Nevertheless, the vast

majority of current research has focused on biocrude emulsification, with limited attention paid to the emulsification of distillates.

For the first time, a novel strategy coupling fractional distillation and emulsification using ultrasonification, was applied to upgrade HTL biocrude into renewable diesel in this study. Specifically, the effects of emulsification temperature, reaction time, and the fraction of distillate addition were explored, and physicochemical and thermal properties of the emulsions were evaluated. Following the distillate emulsification, this study extended to the emulsification of biocrude under the optimal conditions, allowing for a comprehensive comparison of their application potential, as well as carbon and energy recoveries. Furthermore, the thermal and oxidation stability of both emulsions were evaluated through accelerated aging tests. The characteristics and qualities of distillate emulsion and biocrude emulsion were comparatively analyzed, and the reactions and mechanisms of emulsion breaking during storage were investigated. Information obtained here could advance our understanding of the emulsification process and pave the way for the full exploitation of HTL biocrude as transportation fuels.

## 2. Materials and methods

### 2.1. Pilot HTL and fractional distillation of biocrude oil

Pilot scale HTL experiments were conducted using a 28.88 L continuous plug-flow reactor [33] at an average temperature of 280 °C and an average retention time of 60 min. The food waste feedstock was collected from a food processing plant in Champaign, IL and its biochemical composition is summarized in Table 1 [11]. The HTL product was released into product collection tanks and the biocrude oil naturally phase separated from the aqueous phase without adding any extraction solvents. Distillation was conducted under atmospheric pressure as described in previous study [29]: the biocrude oil was charged into a round-bottom flask which was wrapped with glass wool to reduce heat loss. A J-type thermocouple was inserted into the top of the column to measure the temperature of the vapor leaving the flask and entering the condenser. The flask was heated with a 1000 mL analog magnetic stirrer heating mantle (BIPEE, Model number: 98-2-B-1000), and the heating rate was set at approximately 2.5 °C/min. The condensed product was dripped into a collection flask, and the products distilled at 150–300 °C were collected as distillate for future use.

### 2.2. Emulsification setup, and storage stability tests

Building on the previous work [18], ultrasonification was employed for emulsification as it helps to increase the solubility of distillate in

**Table 1**

Properties of food waste, HTL biocrude, commercial diesel, and the distribution of HTL products.

Properties	Food waste	Biocrude	Diesel
Protein (wt%)	2.34 ± 0.06	–	–
Lipid (wt%)	65.50 ± 4.31	–	–
Ash (wt%)	6.12 ± 0.57	–	–
Carbohydrate (wt%)*	26.05 ± 4.82	–	–
C (wt%)	60.94 ± 4.53	65.33 ± 1.67	86.18 ± 0.08
H (wt%)	8.27 ± 0.82	10.48 ± 0.23	13.44 ± 0.04
N (wt%)	0.70 ± 0.13	0.70 ± 0.14	0.35 ± 0.03
O (wt%)*	30.09 ± 5.21	23.49 ± 1.95	0.04 ± 0.01
HHV (MJ/kg)	27.74 ± 3.11	32.59 ± 1.03	45.93 ± 0.01
Acidity (mg KOH/g)	–	130.27 ± 4.99	0.24 ± 0.001
Viscosity (mm <sup>2</sup> /s) at 22 °C	–	64.55 ± 0.61	3.81 ± 0.01
Density (g/mL)	–	0.995 ± 0.007	0.842 ± 0.002
HTL Product Yield			
Biocrude (wt%)	68.45 ± 0.78		
Solid (wt%)	21.82 ± 1.48		
Aqueous (wt%)	9.73 ± 2.26		
Gas (wt%)	–		

\*Calculated by difference.

commercial diesel and improve the stability of the emulsion. Taguchi method was used to design the emulsification experiments of fractional distillate and commercial diesel. Particularly, the effects of distillate fraction, emulsification temperature, and retention time were investigated with three levels for each parameter (Table 2). A Kendal Ultrasonic Cleaner (model HB-S-49DHT) was used to employ ultrasonification. Atlox 4912 (Croda International, USA) was used as surfactant, which is a polymeric, non-ionic surfactant that has a solid form and a hydrophilic-lipophilic balance value of 6 [18]. Surfactant fraction was 5 wt% for all groups. Commercial No.2 diesel was used as the base fuel, which was obtained from a local gas station in Champaign, IL.

Following the distillate emulsification, emulsification of biocrude oil was then conducted according to the optimal condition with the distillates: 45 °C, 30 min, 10 wt% biocrude fraction, 5 wt% surfactant fraction (to be consistent with group 4). After emulsification, the mixtures were centrifuged at 4000 rpm for 15 min to facilitate fast separation. The resulting two layers were a dark, solid fraction of insolvable biocrude precipitated at the bottom; and a lighter-colored liquid layer of emulsified biocrude in diesel, which was collected separately as the emulsion sample. The biocrude solubility (wt%) in emulsion is calculated by

$$S(\text{wt}\%) = (m_0 - m_f)/m_0 \times 100\%$$

where  $m_0$  is the initial mass of biocrude,  $m_f$  is the final mass of the solid, insolvable fraction after centrifugation, and  $m_0 - m_f$  represents the diesel-soluble fraction of biocrude in the emulsion.

The oxidation and thermal stabilities of the emulsion fuels were determined with accelerated aging test [34]: the distillate and biocrude emulsions were placed in small, sealed glass vials and stored at 80 °C for 5 days. The homogeneities were analyzed after the aging test to determine if phase separation had occurred.

### 2.3. Analytical methods

The elemental composition carbon (C), hydrogen (H), and nitrogen (N) were measured using a CE440 element analyzer (Exeter Analytical, North Chelmsford, MA), and sodium (Na), calcium (Ca), potassium (K), and sulfur (S) were measured using a PerkinElmer ICP-MS (Model NexION 350D). Oxygen (O) content was calculated by difference, and the higher heating value (HHV) was calculated based on Dulong's formula

$$\text{HHV} \left( \frac{\text{MJ}}{\text{kg}} \right) = 0.3516 \times \text{C} + 1.16225 \times \text{H} - 0.1109 \times \text{O} + 0.0628 \times \text{N}$$

The acidity (total acid number) of the samples were determined via color-indicator titration according to ASTM D974-12 [35]. The oil samples were dissolved in a mixture of toluene and isopropyl alcohol containing a small amount of water, and the resulting single-phase solution is titrated at room temperature with standard KOH solution. The end point was indicated by the color change of the added *p*-Naphtholbenzein solution from orange to green-brown. The amount of KOH added per gram oil was utilized to determine the total acid number.

**Table 2**  
Taguchi design of the emulsification of fractional distillate.

Group	Temperature (°C)	Distillates fraction (wt%)	Time (min)
1	30	10	10
2	30	20	30
3	30	30	50
4	45	10	30
5	45	20	50
6	45	30	10
7	60	10	50
8	60	20	10
9	60	30	30

The kinetic viscosity of the oil samples was determined using a Cannon-Fenske routine viscometer at 22 °C according to ASTM D446-12 [36]. The viscosity index (VI) of the aged distillate and biocrude emulsions was determined [15] as

$$VI = \frac{\mu_{t2} - \mu_{t1}}{\mu_{t1}}$$

where  $\mu_{t1}$  is the viscosity at time  $t_1$  (before storage test) and  $\mu_{t2}$  is the viscosity at time  $t_2$  (after storage test). The lower the VI, the more stable the fuel, and a perfectly stable fuel has a VI of 0.

Thermal properties and boiling point distribution were obtained via thermogravimetric analysis (TGA) with a Q50 thermogravimetric analyzer (New Castle, DE, USA). Approximately 15 mg of each sample was tested, samples were heated from room temperature to 600 °C at a ramp temperature of 20 °C/min under a nitrogen flow rate of 60 mL/min. The calculated cetane index (CCI) was determined according to ASTM D4737-21 [37]:

$$CCI = -399.90D + 0.1113 \times T_{10} + 0.1212 \times T_{50} + 0.0627 \times T_{90} + 309.33$$

where D is the density at 15 °C,  $T_{10}$ ,  $T_{50}$ ,  $T_{90}$  are recovery temperature of the fuel at which a certain percentage of the fuel was volatilized. For example, a  $T_{10}$  value of 100 °C indicates that at 100 °C 10% of the fuel weight was volatilized.

Cold flow properties of the fuel blends were determined by differential scanning calorimetry (DSC) analysis with a DSC2500 analyzer. Approximately 8 mg of each sample was tested, samples were first equilibrated at 50 °C, then cooled from 50 °C to -100 °C at a cooling rate of 10 °C/min, and lastly heated from -100 °C to 50 °C, all under a nitrogen flow rate of 50 mL/min. The pour point and cloud point were determined according to the cooling curve that the onset temperature of crystallization is estimated as cloud point, and the onset temperature of solidification is estimated as pour point.

The mass distribution was analyzed via matrix-assisted laser desorption/ionization mass spectrometry (MALDI-MS) using a Bruker AutoFlex Speed LRF instrument (Bruker Scientific Instruments; Germany) with dual microchannel plate detectors for both linear and reflection modes. 2,5-Dihydroxybenzoic acid (DHB) was used as the matrix reagent, and the compounds with mass range of 0–1000 Da were detected.

Mass yield, carbon recovery, and energy recovery are calculated by

$$M = \frac{m_f}{m_0}, C_r(\%) = M \times \frac{C_f}{C_0}, E_r(\%) = M \times \frac{HHV_f}{HHV_0}$$

where  $m_f$ ,  $C_f$ ,  $HHV_f$  are the mass, carbon content, and HHV of the biocrude/distillate emulsion, and  $m_0$ ,  $C_0$ ,  $HHV_0$  are the mass, carbon content, and HHV of the initial biocrude/distillate.

## 3. Results and discussion

### 3.1. Emulsification of distillates

The elemental composition of biocrude, distillate, and the distillate emulsion blends were tested (Table 3). Distillation significantly removed the oxygen content in biocrude and increased the carbon content. The high oxygen content of biocrude is a primary difference between biocrude with petroleum crude and the main reason for its relatively low HHV. The oxygen content indicates the abundance of oxygenated compounds in biocrude oil: the higher the oxygen content, the higher the polarity of a biocrude, and therefore the lower the miscibility with petroleum oil; and the more oxygenated the compounds, the less stable the biocrude [28,38,39]. In addition, the H:C ratio reduced after distillation, indicating the aromatic and unsaturated compounds were concentrated into the distillate, which needs to be further treated. The nitrogen content was also reduced in the distillate compared to

**Table 3**

Elemental composition, HHV, and physicochemical properties of the biocrude, distillate, diesel, surfactant, and distillate emulsions.

Group	C (wt%)	H (wt%)	N (wt%)	O (wt%)	HHV (MJ/kg)	Acidity (mg KOH/g)	Viscosity (mm <sup>2</sup> /s) at 22 °C	Density (g/mL)
Biocrude	65.33 ± 1.67	10.48 ± 0.23	0.70 ± 0.14	23.49 ± 1.95	32.59 ± 1.03	130.27 ± 4.99	64.55 ± 0.61	0.995 ± 0.007
Distillate	77.16 ± 0.50	11.73 ± 0.08	0.51 ± 0.01	10.62 ± 0.59	39.61 ± 0.33	96.38 ± 0.44	9.20 ± 0.07	0.888 ± 0.009
Diesel	86.18 ± 0.08	13.44 ± 0.04	0.35 ± 0.03	0.04 ± 0.01	45.93 ± 0.01	0.24 ± 0.001	3.81 ± 0.01	0.842 ± 0.002
Surfactant	68.53 ± 0.06	10.94 ± 0.10	0.40 ± 0.17	20.13 ± 0.33	34.60 ± 0.18	—	—	—
1	79.78 ± 1.34	12.38 ± 0.22	0.58 ± 0.13	7.27 ± 1.44	41.66 ± 0.88	13.36 ± 0.63	6.20 ± 0.45	0.858 ± 0.002
2	81.62 ± 0.76	12.65 ± 0.09	0.50 ± 0.03	5.24 ± 0.82	42.84 ± 0.46	23.51 ± 0.30	6.03 ± 0.43	0.860 ± 0.009
3	80.08 ± 1.60	12.43 ± 0.18	0.48 ± 0.01	7.01 ± 1.80	41.86 ± 0.98	35.18 ± 0.53	6.77 ± 0.09	0.861 ± 0.001
4	82.08 ± 1.11	12.64 ± 0.23	0.53 ± 0.02	4.76 ± 1.32	43.05 ± 0.80	13.71 ± 0.05	5.81 ± 0.04	0.856 ± 0.004
5	79.69 ± 1.02	12.36 ± 0.14	0.43 ± 0.01	7.52 ± 1.17	41.58 ± 0.65	21.74 ± 1.59	6.50 ± 0.14	0.861 ± 0.001
6	81.58 ± 0.04	12.59 ± 0.02	0.49 ± 0.06	5.35 ± 0.01	42.75 ± 0.03	32.24 ± 2.12	6.90 ± 0.27	0.857 ± 0.001
7	80.75 ± 0.18	12.54 ± 0.03	0.52 ± 0.09	6.20 ± 0.30	42.31 ± 0.13	12.47 ± 1.80	5.36 ± 0.42	0.854 ± 0.002
8	81.87 ± 0.47	12.62 ± 0.11	0.46 ± 0.01	5.05 ± 0.60	42.92 ± 0.37	24.02 ± 2.03	5.96 ± 0.29	0.861 ± 0.001
9	81.59 ± 1.18	12.59 ± 0.19	0.66 ± 0.05	5.17 ± 1.32	42.78 ± 0.78	33.83 ± 0.12	6.57 ± 0.02	0.862 ± 0.001

biocrude, which is consistent with previous findings that most of the nitrogen-containing compounds were concentrated into the distillation residue (biochar) [29]. Emulsification of distillates with diesel further lowered the O:C atomic ratio, while increased the H:C ratio as well as HHV values. These improvements make the emulsion fuel properties closer to the commercial diesel. Detailed impacts of emulsification temperature, retention time, and the fraction of distillates on the elemental composition and the HHV is presented in Table 3 and Fig. 1. Increasing temperature reduced the O:C ratio from 0.061 to 0.050, and a 30 min reaction time had the best oxygen reduction performance. Due to the abundant short chain hydrocarbons, diesel has a higher H:C ratio than distillate, emulsification with diesel could help dilute the unsaturated compounds in distillate and increase the hydrogen content of the

emulsion. The nitrogen content in distillate is relatively low, and the changes in N:C ratio is less distinct after emulsification, the lowest N:C ratio was achieved with a reaction temperature of 45 °C. The reduce in oxygen content and increase in carbon content after emulsification led to the increase in the HHV of the emulsion blends. The HHV is most sensitive to the emulsification time, specifically, a temperature of 60 °C and reaction time of 30 min resulted in the highest HHV.

In addition to the elemental composition, physicochemical properties were also improved after distillation, leading to the distillate with a lower acidity, viscosity, and density, which is consistent with previous reports [40,41]. The high acidity of the biocrude was due to the abundant fatty acid derivatives, making it unsuitable to be directly used as fuel. Distillation reduced the acidity of biocrude from 130.27 to 96.38

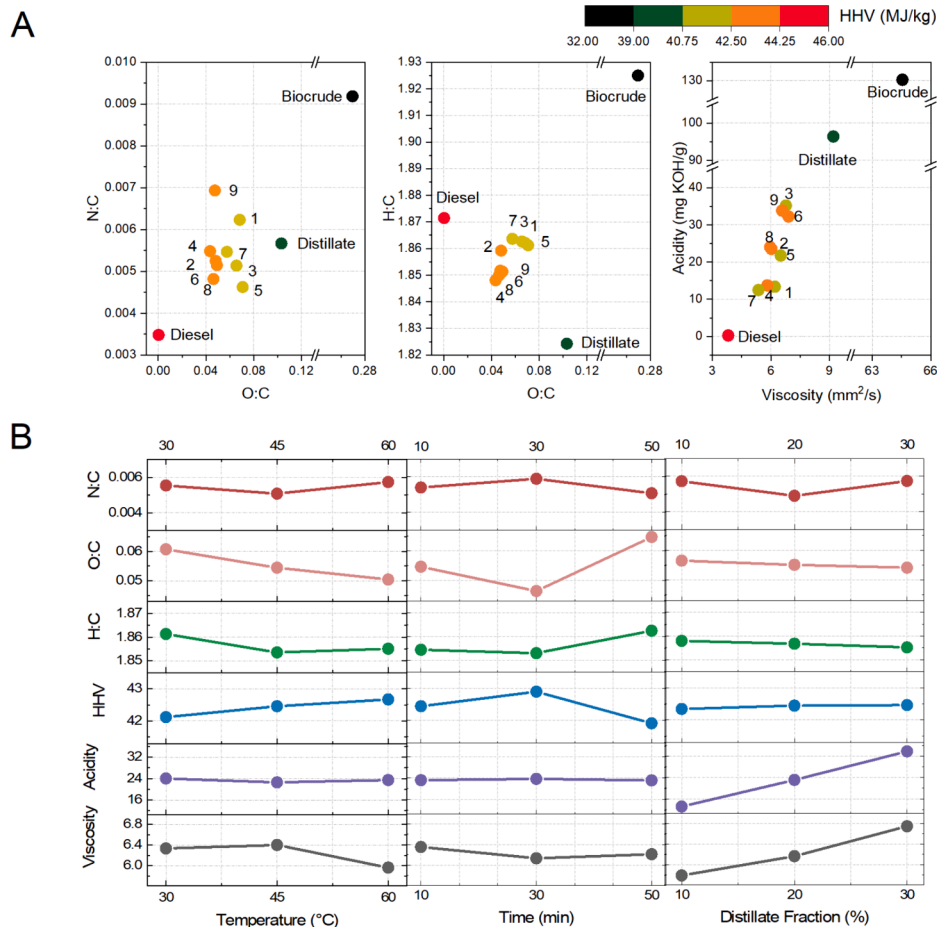


**Fig. 1.** Van Krevelen diagram of N:C, O:C, and H:C ratios, acidity, viscosity, and HHV of emulsion fuels, distillate, biocrude, and diesel (A); and the mean of response for atomic ratios, HHV, acidity and viscosity of emulsion fuels at various reaction temperature, time, and distillate fraction (B).

mg KOH/g. The viscosity was also significantly reduced from 64.55 to 9.20 mm<sup>2</sup>/s after distillation, which could be explained by the changes in intermolecular forces of the distillate composition and the changes in the concentration and length of aliphatic compounds [29]. The decrease in density of biocrude after distillation could be attributed to the decreased water content. Furthermore, the changes in the physico-chemical properties during distillate emulsification was monitored (Table 3, Fig. 1). Mixing with diesel brought more low molecular weight compounds, therefore lowered the acidity, viscosity, and density of all

emulsion samples. Specifically, the acidity of the emulsion fuel was most sensitive to the distillate fraction, while was relatively stable with different emulsification temperature and reaction time. As for the viscosity, a reaction temperature of 60 °C and retention time of 30 min led to the lowest viscosity. To have better fuel properties, the fuel blends should have as high HHV, and as low acidity and viscosity as possible, thus, ultrasonic emulsification reaction at 45 °C, 30 min, with 10 wt% distillate fraction (group 4) was selected as the optimal condition.

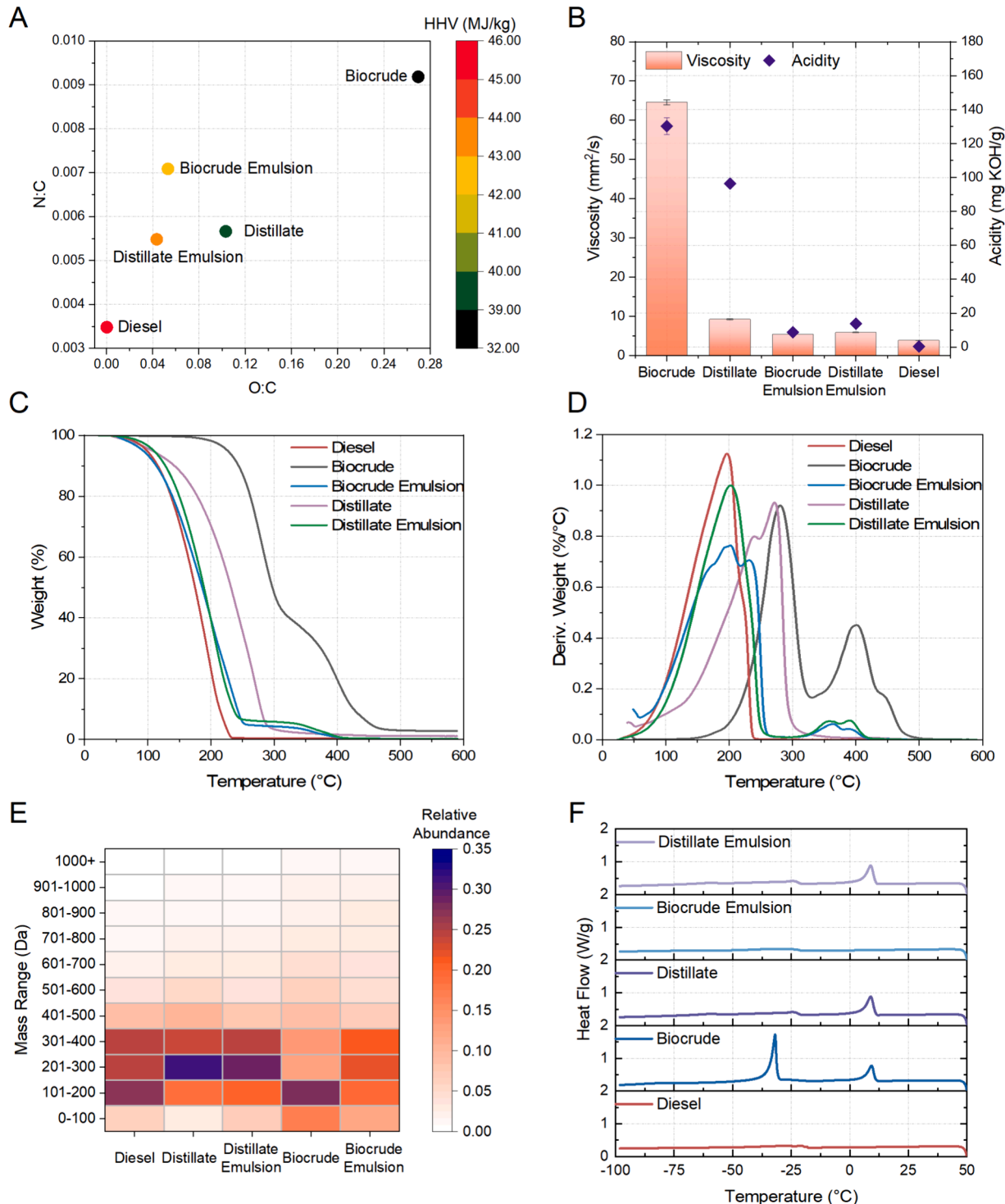


**Fig. 2.** N:C, O:C ratios, and HHV (A); acidity and viscosity (B); thermal properties (C and D), weight distribution of compounds (E), and cold flow properties (F) of diesel, biocrude, distillate, biocrude emulsion, and distillate emulsion.

### 3.2. Comparison of distillate and biocrude emulsification for renewable diesel production

To further evaluate the emulsification performances, emulsification of biocrude with diesel was conducted under the optimal conditions (e.g., 45 °C, 30 min, 10 wt% biocrude fraction, consistent with group 4). The miscibility of distillate was good in all experimental groups that 100 wt% of the distillate were dissolved into the diesel blends during emulsification. However, only part of the biocrude was dissolved into the diesel, and the solubility of biocrude into the fuel blends is 34.80 wt %. Elemental composition and physicochemical properties of the biocrude emulsion were determined (Fig. 2A, 2B, Table 4). Compared to the distillate emulsion, biocrude emulsion has higher oxygen and nitrogen content, lower carbon content, and lower HHV value, which are consistent with the differences between biocrude and distillate. Emulsification significantly reduced the acidity and viscosity of the biocrude, the resulting emulsions of both biocrude and distillate showed comparable acidity and viscosity to the diesel fuel. The sodium, calcium, potassium, and sulfur contents in biocrude, distillate, and their emulsions were also determined (Table 4). Distillation exhibited great performance in removing metal elements from crude oil, sodium concentration was significantly reduced from 260 to 60 ppm, and potassium content was lowered from 60 to 40 ppm. Emulsification further diluted the concentration of the metal elements, and in particular, the sulfur content was reduced to 30 ppm, meeting the requirements for diesel grade B6-B20 S500. High concentration of the metal elements is not favorable for fuel blends as they could have corrosive effects on the exhaust catalysts and after treatment systems, while sulfur can affect the behavior of emission control systems [42].

Thermal properties and boiling point distribution of biocrude, distillate, and their emulsions were characterized via TGA analysis (Fig. 2C, 2D, Table 5). The results showed clear variations among the samples. The initial boiling point of biocrude was recorded at 162.30 °C, indicating that biocrude contained chemical compounds recalcitrant to vaporization. It has two major weight loss peaks in the DTG curve, the first from 200–350 °C and the second from 350–500 °C. After distillation, the initial boiling point dramatically decreased to 47.43 °C, there was only one major weight loss peak observed within 200–300 °C range, and 98.04 % of the compounds in distillate have the boiling point lower than 360 °C. It is worth noting that the commercial diesel is characterized by its composition of hydrocarbons predominantly with carbon numbers in the range of C9–C20 and boiling point of 163–357 °C [43]. The differences in boiling point distribution between biocrude and distillate proved that distillation have effectively removed most of the heavy fraction compounds in the biocrude, and a great portion of the distillate fraction has fallen into the diesel range, although it is still heavier than the commercial diesel oil used in the study. After ultrasonic emulsification, the biocrude emulsion showed a major weight loss within 150–250 °C range and a minor peak from 350–400 °C, indicating the majority of biocrude components dissolved into the emulsion blends were light fractions, while most of the heavy fractions were precipitated and separated out. As for the distillate emulsion, 68.51 % of the weight

**Table 5**

Fuel properties of diesel, biocrude, distillate, biocrude emulsion, and distillate emulsion.

Group	IBP (°C) *	T <sub>5</sub> (°C)	T <sub>10</sub> (°C)	T <sub>50</sub> (°C)	T <sub>90</sub> (°C)	CCI
Diesel	56.78	98.76	115.99	174.98	214.09	20.15
Biocrude	162.30	226.44	244.05	297.55	426.11	1.37
Distillate	47.43	106.99	142.32	232.00	279.35	15.69
Biocrude Emulsion	52.77	92.63	113.79	186.42	241.96	15.45
Distillate Emulsion	61.56	109.57	128.04	189.19	235.91	18.99

\*The initial boiling point (IBP) was assumed to be the temperature when 0.5% of the organic matter volatilized according to the TGA results.

loss occurred at 149–232 °C, which was very similar as the commercial diesel whose weight loss fraction was 71.29 % at the range.

The calculated cetane index (CCI) was then determined based on the boiling point distribution. CCI value indicates the auto-ignition characterized of the tested fuel: the higher the CCI (maximum 100), the closer the tested fuel is to the reference fuel (cetane) and the better the auto-ignition properties [29,37]. CCI value significantly increased from 1.37 to 15.69 after distillation, and emulsification further improve it to 18.99 which is comparable as that of diesel. Biocrude emulsion also shows a relatively high CCI value, which can be explained by that only part of the biocrude has been dissolved into the emulsion blends and are mainly light fractions. It is also worth noted that CCI can be further increased by adding cetane enhancers to achieve the desired cetane number of commercial fuels, which is a common industry practice [44–46].

Weight distribution of components in different fuel blends was further explored with MALDI analysis (Fig. 2E). 28.15 % of the organics in biocrude has a mass range of 100–200 Da, and 19.31 % of the compounds has a mass range larger than 500 Da, the organic distribution in biocrude is relatively uniform. Distillation removed the heavy fractions from biocrude, and make the organic weight centered into 200–400 Da, with the accumulation of saturated/unsaturated hydrocarbons and fatty acids. Molecules in 200–300 Da accounted for 31.41 % of the compounds in distillate, and the fraction with mass range larger than 500 Da has been shrunken by 33.65 % from biocrude after distillation. Nevertheless, some light fractions in the biocrude were lost during the distillation process. In comparison, abundant small molecules with 100–200 Da were observed in diesel, and the weight distribution within 100–400 Da is relatively uniform. Emulsification of distillate and diesel helped to fill in this gap, make the weight distribution of emulsion blends more uniform, and shares similar pattern as the commercial diesel. In comparison, the biocrude emulsion still contains a lot of heavy fractions.

The evaluation of cold flow properties is very important in assessing fuel performances, preventing fuel gelling during cold weather conditions, and ensuring proper pumpability into the engine. DSC analysis was conducted to determine the cold flow properties of biocrude, distillate, and their emulsions, results are depicted in Fig. 2F. The cold flow characteristics are mainly related to the saturated and unsaturated

**Table 4**

Physicochemical properties, and elemental composition (particularly metal elements and sulfur contents) of biocrude, distillate, and their emulsions.

Group	Acidity (mg KOH/g)	Viscosity (mm <sup>2</sup> /s) at 22 °C	Density (g/mL)	C (wt%)	H (wt%)	N (wt %)	O (wt%)	HHV (MJ/kg)	Na (ppm)	Ca (ppm)	K (ppm)	S (ppm)
Biocrude	130.27 ± 4.99	64.55 ± 0.61	0.995 ± 0.007	65.33 ± 1.67	10.48 ± 0.23	0.70 ± 0.14	23.49 ± 1.95	32.59 ± 1.03	260	UD	60	80
				0.009	0.50	0.08	0.01	0.59	60	UD	40	60
Distillate	96.38 ± 0.44	9.20 ± 0.07	0.888 ± 0.009	77.16 ± 0.50	11.73 ± 0.08	0.51 ± 0.01	10.62 ± 0.59	39.61 ± 0.33	60	UD	40	60
				0.004	0.90	0.08	0.01	0.99	110	UD	40	30
Biocrude Emulsion	8.64 ± 0.20	5.40 ± 0.23	0.861 ± 0.004	81.02 ± 0.90	12.57 ± 0.08	0.67 ± 0.01	5.75 ± 0.99	42.50 ± 0.52	70	UD	30	30
			0.856 ± 0.004	82.08 ± 1.11	12.64 ± 0.23	0.53 ± 0.02	4.76 ± 1.32	43.05 ± 0.80				

UD: Under detection limit.

fatty acid esters. To avoid poor cold weather performance, diesel must contain a high concentration (80–90 wt%) of unsaturated long-chain fatty acid alkyl esters [47]. Saturated esters tend to crystallize more readily than unsaturated ones, leading to engine filter blockages and eventual engine failure [48,49]. In Fig. 2F, the DSC curve of biocrude reveals two distinct regions: the first exhibiting a small peak between 0 to 15 °C, which could be corresponding to freezing of saturated fatty acids methyl esters; and the second displaying a large peak between –30 to –40 °C, which could be associated with freezing of methyl esters of unsaturated fatty acids [50]. Distillation greatly reduced the freezing peak at –30 to –40 °C, while the changes in the high temperature peaks were minor, indicating that the majority of the unsaturated fatty acids were removed. This is consistent with that the H:C ratio of heavy fractions and distillate residue are lower than that of light fractions, indicating the unsaturated and aromatic compounds tended to concentrate into the heavier fractions [28]. Although the removal of unsaturated fatty esters contributed to a lowered acidity of distillate, the presence of saturated fatty esters still posed challenges for its utilization in fuel blends. In terms of the diesel, there was only one tiny crystallization region observed between –15 to –40 °C, and the cloud point and pour point are at –16.30 °C and –26.82 °C, respectively, according to the DSC results. The tiny freezing peak indicated the low concentration of fatty acid esters and was consistent with the low acidity.

Comparing biocrude and its emulsion, an absence of the high temperature freezing peak was observed, and the low temperature peak was dramatically decreased, bringing the DSC curve into close alignment with that of diesel fuel. This shift can be attributed to the low solubility of biocrude that most of the fatty acid esters were not melted into the emulsion. Singh et al. found that when the food waste biocrude concentration in commercial diesel was low (10 vol%), precipitation occurred, whereas no precipitation was observed at higher biocrude concentration of 20 vol% or even 50 vol% [23]. Similarly, Langauer et al. reported that the solubility of the emulsion improved significantly with increased amounts of biocrude [21]. In this study, the biocrude concentration in the fuel blend is low at 10 wt% and the solubility is 34.80 wt%. With relatively high molecular weight, most of the fatty acid esters are diesel insoluble, and were separated out after emulsification, resulting in a cooling curve similar to that of diesel. In comparison, all the distillates, including the esters, dissolved into the diesel, making the cooling curve of distillate emulsion display an integrated characteristics of both distillate and diesel, containing high and low temperature freezing regions. Emulsification did not significantly dilute the saturated fatty acid esters in distillate, and the cold flow property is still relatively poor due to their high melting point. The cooling results are also

consistent with that the acidity of distillate emulsion remained high, the acids in fuel could lead to corrosion of the engine. Therefore, additional research efforts are needed to explore advanced acid removal or conversion techniques to enhance the overall quality of the distillate emulsion and meet the standards and specification of diesel blends.

Carbon and energy recoveries of the two emulsion fuels were calculated, as depicted in Fig. 3. During fractional distillation, 83.41 % and 85.84 % of the carbon and energy from the biocrude flowed into the distillate, while the heavy fractions were separated out as the form of biochar (solid residue). The enhanced quality of the distillate improves its miscibility with diesel, and carbon and energy recoveries of 88.72 % and 93.29 % were achieved through emulsification with diesel. In contrast, despite the one-step operation, the miscibility issue resulted in the low solubility of biocrude in diesel, leading to the low carbon and energy recoveries of 43.16 and 45.38 %, respectively. These findings demonstrated that the combination of emulsification and distillation could be an energy efficient and economically feasible approach. Compared to direct emulsification, this integrated method not only maximizes the utilization of biocrude but also improves the quality and stability of the resulting fuel blend.

Moreover, the coupling of distillation and emulsification shows clear superiority when contrasted with other typical upgrading technologies such as hydrotreating and hydrocracking (Table 6). The yield of hydrotreated oil is usually low, ranging from 12–28 % through catalytic hydrocracking and 21–65 % by hydrotreating (hydro-deoxygenation), with significant portions attributed to coke formation accounting for 26–39 % and 4–26 % of the yield, respectively [51,52]. The limited yield of upgraded oil then leads to the low carbon and energy recoveries. For instance, Arun reported a 24.1 % yield of hydrotreated oil with carbon and energy recovery of 25.82 % and 30.35 %, respectively [53]. Similarly, Duan et al. noted a 76 % carbon recovery in oil under catalytically hydrotreatment at 430 °C, whereas the carbon recovery dropped to only 23 % at 530 °C [54]. In addition, hydrotreating/hydrocracking requires stringent conditions including high temperature and hydrogen pressure, making it economically and energetically unfavorable. Energy consumption in upgrading is mainly affected by the operating temperature, and hydrogen gas consumption in deoxygenation and denitrogenation [55,56]. Grange et al. investigated the hydrogen consumption for representative functional groups and molecules, reporting that ketone, carboxylic acid, methoxy phenol, 4-methylphenol, 2-ethylphenol, and dibenzofuran consume 2 H<sub>2</sub>/function, 3 H<sub>2</sub>/function, 6 H<sub>2</sub>/molecule, 4 H<sub>2</sub>/molecule, 4 H<sub>2</sub>/molecule, 8 H<sub>2</sub>/molecule, respectively [57]. Moreover, the hydrogen consumption is positively correlated with the degree of deoxygenation, presumably due

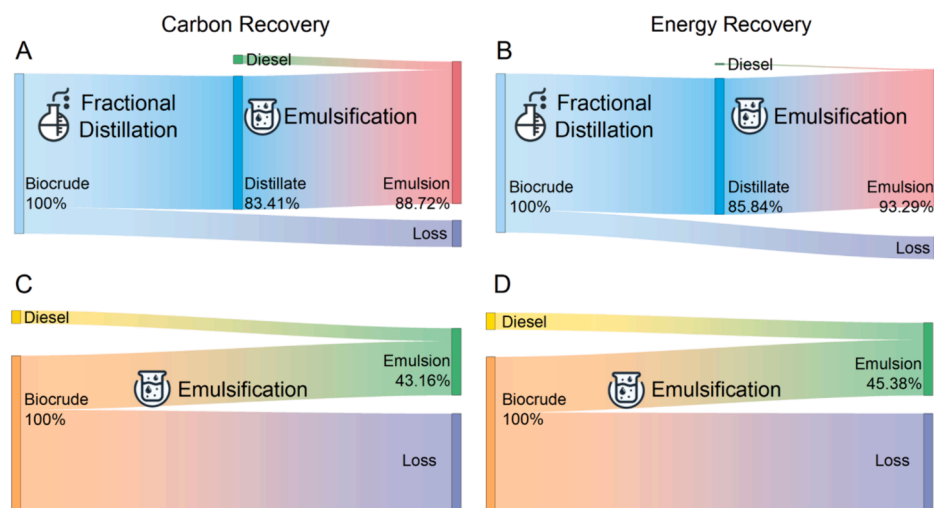


Fig. 3. Carbon and energy recoveries of distillate (A, B) and biocrude (C, D) emulsions.

**Table 6**

Comparison of current technologies for biocrude upgradation [12,28,51,52].

	Hydrotreating	Hydrocracking	Fractional distillation & Emulsification
Operation conditions	300–400 °C, low pressure	350–500 °C, up to 2000 psi	<300 °C, ambient pressure
Chemical and catalyst	H <sub>2</sub> /CO; CoMo, Pd/C, Ru/Al <sub>2</sub> O <sub>3</sub> etc.	H <sub>2</sub> /CO; zeolite etc.	N/A
Energy consumption	Medium	High	Low
Oil yield (wt%)	21–65	12–28	60–80
Pros.	1. Efficient removal of heteroatoms 2. Generation of large quantities of light products		1. Simple process without chemical reactions 2. Maximize the utilization of bio-oil 3. Energy efficient
Cons.	1. Low product selectivity (undesirable coke and gas production instead of oil) 2. High costs associated with catalysts and hydrogen usage; short catalyst lifetime		1. Heteroatom content remains high

to the different reactivity of biocrude compounds that highly reactive compounds like ketones can be easily converted with low hydrogen consumption [51,58]. Compared to hydrotreating and hydrocracking, distillation-emulsification can be operated under mild reaction conditions without the aid of hydrogen gas, it is simpler to operate, cost-effective, and more sustainable from an energy perspective.

### 3.3. Oxidation and thermal stability of distillate and biocrude emulsions

Oxidative and storage stabilities are important parameters in evaluating fuels, as instability affects the proper use of fuels [59,60]. The formation of sediments is a serious instability problem during storage and the sediment content in diesel has a maximum limit of 0.05 vol% according to the fuel quality standard [42]. In this study, the oxidation and thermal stabilities of the emulsion fuels were assessed through an accelerated aging test. Both biocrude and distillate emulsions underwent storage at 80 °C for 5 days, which was equivalent to a 1-year storage at room temperature [34]. During the aging test, sedimentation occurred at the bottom of the biocrude emulsion tube, and the aged emulsion had a lighter color than the original one (Fig. 4A). Specifically, an average of 14.37 wt% of the biocrude emulsion has separated out. The phase separation can be attributed to that part of the high molecular weight compounds precipitated during the storage due to their immiscibility properties in diesel, leading to the instability of the heavy fraction [61]. In contrast, there was no visible sedimentation observed in the distillate emulsion.

The physiochemical properties of the emulsion fuels were monitored during storage (Fig. 4B). The change in viscosity serves as a significant indicator of fuel stability. Over the storage period, both biocrude and distillate emulsions experienced an increase in viscosity. Calculating the viscosity index using values before and after the storage tests revealed that the distillate emulsion exhibited a lower viscosity index (0.196) than the biocrude emulsion (0.609), indicating its superior stability for long term storage. Acidity changes were also monitored, revealing a decrease in acidity for the distillate emulsion. This decrease should be associated with the polymerization and esterification of the fatty acids during storage. In contrast, the acidity of biocrude emulsion increased, it can be explained by that the esters were oxidized to form peroxides, which was then converted to acids; fatty acids can also be produced from the hydrolysis of fatty acids methyl esters, leading to the increased acidity [62]. Moreover, an increased fraction of heavy compounds with a boiling point higher than 343 °C (primarily lubricating oils, fuel oils, and residue) was observed in biocrude emulsion, due to the polymerization reactions during storage. While the boiling point distribution of distillate emulsion did not present significant changes (Fig. 4C).

The fatty acid composition of the ester molecule is the most important factor influencing the properties of emulsion fuels during long term storage, and the unsaturation in the molecule accounts for instability. Unsaturated esters are significantly more reactive to oxidation than the saturated ones, and for long chain fatty acid methyl esters (C<sub>18</sub>), polyunsaturated esters are twice as reactive to oxidation as monounsaturated ones [47]. The mechanism for the oxidation of unsaturated esters is

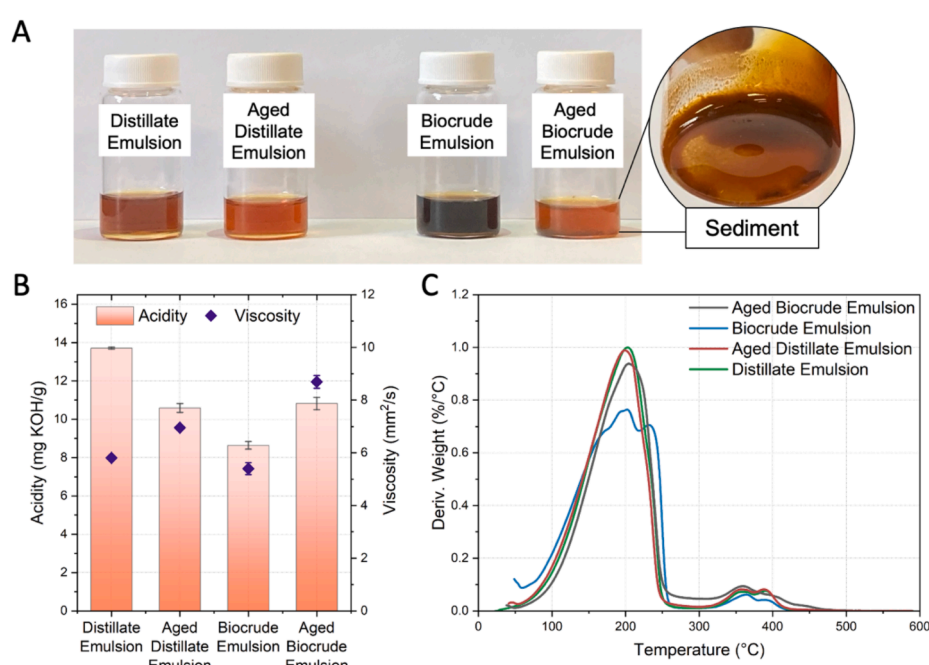


**Fig. 4.** Biocrude and distillate emulsions before and after the aging test (A), changes in their physicochemical properties (B), and boiling point distributions (C).

presented in Fig. 5A. The oxidation commonly starts at the allylic positions to double bonds (circled in red in the figure), thus the position and number of the allylic and bis-allylic methylene moieties adjacent to the double bond determines the rate of oxidation. Auto-oxidation is a major source of oxidation, which is a radical chain reaction, resulting in the formation of peroxides and hydroperoxides. The hydroperoxides formed are rather unstable, they can undergo several different secondary reactions, leading to a wide range of products. One most important reaction is  $\beta$ -cleavage, leading to the formation of several decomposition products including aldehydes, ketones, and acids. These compounds can further go through dimerization and polymerization to form higher molecular weight compounds [63]. Another possible reaction of hydroperoxides is epoxidation, resulting in the formation of epoxides, which would then go through cleavage and polymerization to generate higher molecular compounds [64,65]. By removing the unsaturated fatty acids esters from biocrude, distillation significantly enhanced the oxidation resistance and stability of the oil. In addition, metal elements have been reported to act as catalysts for polymerization [66], while nitrogen-containing compounds are prone to forming high molecular weight complex chemicals through condensation, negatively impacting stability during long-term storage [67]. The reduction of metal and nitrogen contents via distillation contributed to the enhanced stability, preventing property and phase changes in the fuel.

At the macro level, the stability of emulsions depends on two competing processes: the migration of the surfactant at the droplets interface (stabilizing process), and the droplets coalescence (destabilization process). The mechanisms of emulsion breaking would go through several consecutive and parallel steps, including creaming/sedimentation, Ostwald ripening, flocculation, coalescence, and finally reached the phase separation [15]. As shown in Fig. 5B, droplets in the stable emulsion became aggregated to each other if the repulsion potential was too weak, leading to the flocculation; two single droplets were separated by a thin film, the thickness of the thin film was decreasing due to the Van der Waals attraction, and when the size of the film reached a critical value, the film ruptured and the two droplets merged into one, which is known as coalescence; meanwhile the droplets rose to the top or sank to the bottom due to the differences in density of the dispersed (biocrude oil or distillate) and continuous phase (diesel), resulting in creaming or sedimentation; the flocculation and

coalescence process led to larger and larger droplets until a phase separation has occurred [15]. In this study, the differences in chemical composition between biocrude and diesel are much greater than those between distillate and diesel. 97.82 % of the components in distillate are light fraction with boiling point lower than 343 °C (mainly gasoline, kerosene, diesel), which is very similar to that of diesel (99.64 %). According to the theory of solubility based on chemical polarity, these low molecular weight light fractions can be easily dissolved into the diesel, and these diesel-soluble fraction can be relatively stable in the emulsion system during storage. However, that light fraction only accounted for 63.19 % of the biocrude composition, with the remaining 36.81 % being high molecular weight compounds that are diesel insoluble. These heavy fractions were connected to the hydrophobic group of the surfactant through the hydrogen bond and van der Waals force to make part of them dissolve in the fuel blends. However, they were less stable during storage, and could progressively separate through the flocculation and coalescence process, and eventually achieving phase separation [61,68].

Emulsion fuel is a system with stable kinetics but unstable thermodynamics, the aging test demonstrated that the distillate emulsion exhibits superior thermal and oxidation stability compared to the biocrude emulsion. In further applications, distillation should be considered as an essential step before emulsification to purify the fuel blends, removing undesirable compounds and enhancing the homogeneity of the fuel.

#### 4. Conclusions

This study systematically evaluated the integration of fractional distillation and emulsification for upgrading HTL biocrude to produce renewable diesel blends. The effects of ultrasonic emulsification temperature, time, and distillate fraction were initially investigated with distillates and commercial diesel. Results showed that optimal emulsification occurred at 45 °C, 30 min, and a 10 wt% distillate fraction, resulting in superior performance with higher HHV, and reduced acidity and viscosity. Under the optimal condition, emulsification of biocrude was then conducted to provide a comparative analysis. The results demonstrated several advantages of the distillate emulsion over biocrude emulsion, including higher HHV, lower concentration of metal elements, improved carbon/energy recovery, and a greater fraction of low molecular weight light fractions. Monitoring the oxidation and

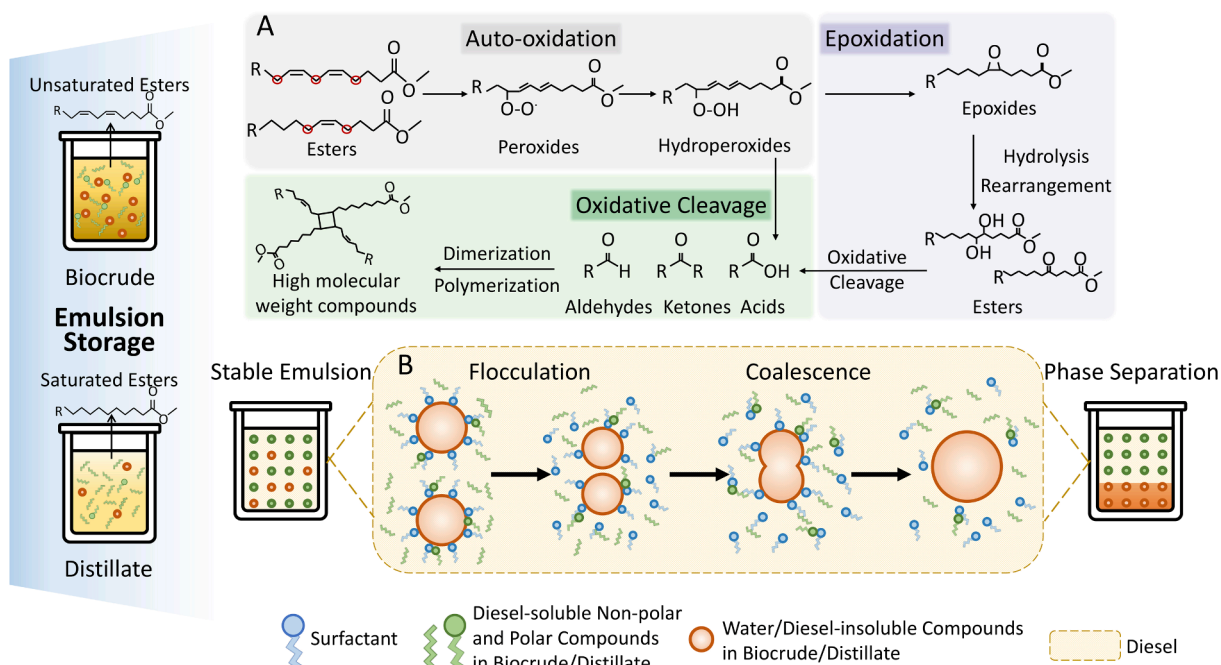


Fig. 5. Mechanisms of ester oxidation (A) and emulsion breaking (B) during storage.

thermal stability of both emulsions highlighted a significant challenge in biocrude emulsion stability, with an average of 14.37 wt% experiencing phase separation. While no sedimentation was observed in distillate emulsion. The findings from this study revealed the pivotal role of distillation as an essential step before emulsification process. Distillation greatly enhanced the stability of biocrude and prevented solubility and precipitation issues, resulting in fuel blends with comparable chemical (HHV, molecular weight), physical (viscosity, density), and thermal (boiling point distribution, CCI) properties to the commercial No.2 diesel. The coupling of fractional distillation and emulsification open new routes for the utilization of HTL biocrude in the production of renewable diesel, illustrating its potential as a viable and sustainable alternative to conventional petroleum diesel fuels.

#### CRediT authorship contribution statement

**Zixin Wang:** Writing – review & editing, Writing – original draft, Investigation. **Buchun Si:** Writing – review & editing, Investigation. **Sabrina Summers:** Writing – review & editing, Investigation. **Yuanhui Zhang:** Writing – review & editing, Supervision.

#### Declaration of competing interest

The authors declare that they have no known competing financial interests or personal relationships that could have appeared to influence the work reported in this paper.

#### Data availability

Data will be made available on request.

#### Acknowledgments

The authors acknowledge the support provided by the National Key R&D Program of China (2022YFE0135600), the National Science Foundation US-China INFEWS grant (NSF # 18-04453 and 1744775).

#### References

- [1] Food and Agriculture Organization of the United Nations, The state of food and agriculture: Moving forward on food loss and waste reduction, 2019.
- [2] Viganó J, Machado APDF, Martínez J. Sub- and supercritical fluid technology applied to food waste processing. *J Supercrit Fluids* 2015;96:272–86. <https://doi.org/10.1016/j.supflu.2014.09.026>.
- [3] Gollakota ARK, Kishore N, Gu S. A review on hydrothermal liquefaction of biomass. *Renew Sustain Energy Rev* 2018;81:1378–92. <https://doi.org/10.1016/j.rser.2017.05.178>.
- [4] Dénil M, Haarlemmer G, Roubaud A, Weiss-Hortala E, Fages J. Energy valorisation of food processing residues and model compounds by hydrothermal liquefaction. *Renew Sustain Energy Rev* 2016;54:1632–52. <https://doi.org/10.1016/j.rser.2015.10.017>.
- [5] Aierzhati A, Stablein MJ, Wu NE, Kuo CT, Si B, Kang X, et al. Experimental and model enhancement of food waste hydrothermal liquefaction with combined effects of biochemical composition and reaction conditions. *Bioresour Technol* 2019;284:139–47. <https://doi.org/10.1016/j.biortech.2019.03.076>.
- [6] Gollakota A, Savage PE. Hydrothermal Liquefaction of Model Food Waste Biomolecules and Ternary Mixtures under Isothermal and Fast Conditions. *ACS Sustain Chem Eng* 2018;6:9018–27. <https://doi.org/10.1021/acscuschemeng.8b01368>.
- [7] Feuerbach S, Toor SS, Costa PA, Paradela F, Marques PAAS, Castello D. Hydrothermal Co-Liquefaction of Food and Plastic Waste for Biocrude Production. *Energies (Basel)* 2024;17. <https://doi.org/10.3390/en17092098>.
- [8] J. Yang Q. (Sophia)He, L. Yang A review on hydrothermal co-liquefaction of biomass *Appl Energy* 250 2019 926 945 10.1016/j.apenergy.2019.05.033.
- [9] Tito E, Marcolongo CA, Pipitone G, Monteverde AHA, Bensaid S, Pirone R. Understanding the effect of heating rate on hydrothermal liquefaction: A comprehensive investigation from model compounds to a real food waste. *Bioresour Technol* 2024;396. <https://doi.org/10.1016/j.biortech.2024.130446>.
- [10] Bayat H, Dehghanizadeh M, Jarvis JM, Brewer CE, Jena U. Hydrothermal Liquefaction of Food Waste: Effect of Process Parameters on Product Yields and Chemistry. *Front Sustain Food Syst* 2021;5. <https://doi.org/10.3389/fsufs.2021.658592>.
- [11] Summers S, Valentine A, Wang Z, Zhang Y. Pilot-Scale Continuous Plug-Flow Hydrothermal Liquefaction of Food Waste for Biocrude Production. *Ind Eng Chem Res* 2023. <https://doi.org/10.1021/acs.iecr.3c01587>.
- [12] Xiu S, Shahbazi A. Bio-oil production and upgrading research: A review. *Renew Sustain Energy Rev* 2012;16:4406–14. <https://doi.org/10.1016/j.rser.2012.04.028>.
- [13] Leng L, Li H, Yuan X, Zhou W, Huang H. Bio-oil upgrading by emulsification/microemulsification: A review. *Energy* 2018;161:214–32. <https://doi.org/10.1016/j.energy.2018.07.117>.
- [14] Lin YY, Chen WH, Liu HC. Aging and emulsification analyses of hydrothermal liquefaction bio-oil derived from sewage sludge and swine leather residue. *J Clean Prod* 2020;266. <https://doi.org/10.1016/j.jclepro.2020.122050>.
- [15] D. Chiaramonti, M. Bonini, E. Fratini, G. Tondi, K. Gartner, A. V. Bridgwater, H.P. Grimm, I. Soldaini, A. Webster, P. Baglioni, Development of emulsions from biomass pyrolysis liquid and diesel and their use in engines-Part 1: emulsion production, 2003. www.sciencedirect.com.
- [16] D. Chiaramonti, M. Bonini, E. Fratini, G. Tondi, K. Gartner, A. V. Bridgwater, H.P. Grimm, I. Soldaini, A. Webster, P. Baglioni, Development of emulsions from biomass pyrolysis liquid and diesel and their use in engines-Part 2: tests in diesel engines, 2003. www.sciencedirect.com.
- [17] McClements DJ. Nanoemulsions versus microemulsions: Terminology, differences, and similarities. *Soft Matter* 2012;8:1719–29. <https://doi.org/10.1039/c2sm06903b>.
- [18] Summers S, Yang S, Watson J, Zhang Y. Diesel blends produced via emulsification of hydrothermal liquefaction biocrude from food waste. *Fuel* 2022;324. <https://doi.org/10.1016/j.fuel.2022.124817>.
- [19] Lin BJ, Chen WH, Budzianowski WM, Hsieh CT, Lin PH. Emulsification analysis of bio-oil and diesel under various combinations of emulsifiers. *Appl Energy* 2016;178:746–57. <https://doi.org/10.1016/j.apenergy.2016.06.104>.
- [20] Rehman SS, Masjuki HH, Kalam MA, Shancita I, Rizwanul Fattah IM, Ruhul AM. Study on stability, fuel properties, engine combustion, performance and emission characteristics of biofuel emulsion. *Renew Sustain Energy Rev* 2015;52:1566–79. <https://doi.org/10.1016/j.rser.2015.08.013>.
- [21] Längauer D, Lin YY, Chen WH, Wang CW, Šafář M, Cablik V. Simultaneous extraction and emulsification of food waste liquefaction bio-oil. *Energies (Basel)* 2018;11. <https://doi.org/10.3390/en11113031>.
- [22] Chong YY, Thangalazhy-Gopakumar S, Ng HK, Ganesan PB, Gan S, Lee LY, et al. Al Hina, Emulsification of bio-oil and diesel. *Chem Eng Trans* 2017;56:1801–6. <https://doi.org/10.3303/CET1756301>.
- [23] Singh D, Jiang X, Jankovic M, Toll F. Improving yields, compatibility and tailoring the properties of hydrothermal liquefaction bio-crude using yellow grease. *Fuel* 2023;344. <https://doi.org/10.1016/j.fuel.2023.128066>.
- [24] Wang XL, Yuan XZ, Huang HJ, Leng LJ, Li H, Peng X, et al. Study on the solubilization capacity of bio-oil in diesel by microemulsion technology with Span80 as surfactant. *Fuel Process Technol* 2014;118:141–7. <https://doi.org/10.1016/j.fuproc.2013.08.020>.
- [25] Guo Z, Wang S, Wang X. Stability mechanism investigation of emulsion fuels from biomass pyrolysis oil and diesel. *Energy* 2014;66:250–5. <https://doi.org/10.1016/j.energy.2014.01.010>.
- [26] Hoffmann J, Jensen CU, Rosendahl LA. Co-processing potential of HTL bio-crude at petroleum refineries - Part 1: Fractional distillation and characterization. *Fuel* 2016;165:526–35. <https://doi.org/10.1016/j.fuel.2015.10.094>.
- [27] Pedersen TH, Jensen CU, Sandström L, Rosendahl LA. Full characterization of compounds obtained from fractional distillation and upgrading of a HTL biocrude. *Appl Energy* 2017;202:408–19. <https://doi.org/10.1016/j.apenergy.2017.05.167>.
- [28] Taghipour A, Ramirez JA, Brown RJ, Rainey TJ. A review of fractional distillation to improve hydrothermal liquefaction biocrude characteristics; future outlook and prospects. *Renew Sustain Energy Rev* 2019;115. <https://doi.org/10.1016/j.rser.2019.109355>.
- [29] Watson J, Si B, Wang Z, Wang T, Valentine A, Zhang Y. Towards transportation fuel production from food waste: Potential of biocrude oil distillates for gasoline, diesel, and jet fuel. *Fuel* 2021;301:121028. <https://doi.org/10.1016/j.fuel.2021.121028>.
- [30] Chen WT, Zhang Y, Lee TH, Wu Z, Si B, Lee CFF, et al. Renewable diesel blendstocks produced by hydrothermal liquefaction of wet biowaste. *Nat Sustain* 2018;1:702–10. <https://doi.org/10.1038/s41893-018-0172-3>.
- [31] Capurton JA, Caredpa SC. Characterization and separation of corn stover bio-oil by fractional distillation. *Fuel* 2013;112:60–73. <https://doi.org/10.1016/j.fuel.2013.04.079>.
- [32] Si B, Watson J, Wang Z, Wang T, Acero Triana JS, Zhang Y. Storage stability of biocrude oil fractional distillates derived from the hydrothermal liquefaction of food waste. *Renew. Energy* 2023;119669. <https://doi.org/10.1016/j.renene.2023.119669>.
- [33] Aierzhati A, Watson J, Si B, Stablein M, Wang T, Zhang Y. Development of a mobile, pilot scale hydrothermal liquefaction reactor: Food waste conversion product analysis and techno-economic assessment. *Energy Conversion and Management* X 2021;10. <https://doi.org/10.1016/j.ecmx.2021.100076>.
- [34] Jiang X, Ellis N. Upgrading bio-oil through emulsification with biodiesel: Thermal stability, in. *Energy Fuel* 2010;2699–706. <https://doi.org/10.1021/ef901517k>.
- [35] ASTM D974 – 12: Standard Test Method for Acid and Base Number by Color-Indicator Titration, ASTM (n.d.). <https://doi.org/10.1520/D0974-12>.
- [36] ASTM D446 – 12: Standard Specifications and Operating Instructions for Glass Capillary Kinematic Viscometers, ASTM (n.d.). <https://doi.org/10.1520/D0446-12>.
- [37] ASTM D4737-21 Standard Test Method for Calculated Cetane Index by Four Variable Equation, ASTM (n.d.). <https://doi.org/10.1520/D4737-21>.

[38] Yang Z, Kumar A, Huhnke RL. Review of recent developments to improve storage and transportation stability of bio-oil. *Renew Sustain Energy Rev* 2015;50:859–70. <https://doi.org/10.1016/j.rser.2015.05.025>.

[39] Anja. Oasmaa, Cordner Peacocke, Valtion teknillinen tutkimuskeskus., A guide to physical property characterisation of biomass-derived fast pyrolysis liquids Technical Research Centre of Finland 2001.

[40] Nam H, Choi J, Capareda SC. Comparative study of vacuum and fractional distillation using pyrolytic microalgae (*Nannochloropsis oculata*) bio-oil. *Algal Res* 2016;17:87–96. <https://doi.org/10.1016/j.algal.2016.04.020>.

[41] Rahman S, Helleur R, MacQuarrie S, Papari S, Hawboldt K. Upgrading and isolation of low molecular weight compounds from bark and softwood bio-oils through vacuum distillation. *Sep Purif Technol* 2018;194:123–9. <https://doi.org/10.1016/j.seppur.2017.11.033>.

[42] ASTM D7467-20a Standard Specification for Diesel Fuel Oil, Biodiesel Blend (B6 to B20) ASTM (n.d.). 10.1520/D7467-20A.

[43] S.C. Gad, Diesel Fuel, Encyclopedia of Toxicology (2005).

[44] Li R, Wang Z, Ni P, Zhao Y, Li M, Li L. Effects of cetane number improvers on the performance of diesel engine fuelled with methanol/biodiesel blend. *Fuel* 2014; 128:180–7. <https://doi.org/10.1016/j.fuel.2014.03.011>.

[45] Musthafa MM. Development of performance and emission characteristics on coated diesel engine fuelled by biodiesel with cetane number enhancing additive. *Energy* 2017;134:234–9. <https://doi.org/10.1016/j.energy.2017.06.012>.

[46] Xing-Cai L, Jian-Guang Y, Wu-Gao Z, Zhen H. Effect of cetane number improver on heat release rate and emissions of high speed diesel engine fueled with ethanol-diesel blend. *Fuel* 2004; p. 2013–20.

[47] Dunn RO. Effect of antioxidants on the oxidative stability of methyl soyate (biodiesel). *Fuel Process Technol* 2005;86:1071–85. <https://doi.org/10.1016/j.fuproc.2004.11.003>.

[48] Ramalho EFSM, Carvalho Filho JR, Albuquerque AR, De Oliveira SF, Cavalcanti EHS, Stragevitch L, et al. Low temperature behavior of poultry fat biodiesel:diesel blends. *Fuel* 2012;93:601–5. <https://doi.org/10.1016/j.fuel.2011.10.051>.

[49] Dunn RO. Thermal analysis of alternative diesel fuels from vegetable oils. *J Am Oil Chem Soc* 1999;76:109–15. <https://doi.org/10.1007/s11746-999-0056-9>.

[50] Garcia-Perez M, Adams TT, Goodrum JW, Das KC, Geller DP. DSC studies to evaluate the impact of bio-oil on cold flow properties and oxidation stability of biodiesel. *Biore sour Technol* 2010;101:6219–24. <https://doi.org/10.1016/j.biortech.2010.03.002>.

[51] Mortensen PM, Grunwaldt JD, Jensen PA, Knudsen KG, Jensen AD. A review of catalytic upgrading of bio-oil to engine fuels. *Appl Catal A Gen* 2011;407:1–19. <https://doi.org/10.1016/j.apcata.2011.08.046>.

[52] Zacher AH, Olarte MV, Santosa DM, Elliott DC, Jones SB. A review and perspective of recent bio-oil hydrotreating research. *Green Chem* 2014;16:491–515. <https://doi.org/10.1039/c3gc41382a>.

[53] Arun J, Gopinath KP, Sivaramakrishnan R, Madhav NV, Abhishek K, Ramanan VK, et al. Bioenergy perspectives of cattails biomass cultivated from municipal wastewater via hydrothermal liquefaction and hydro-deoxygenation. *Fuel* 2021;284. <https://doi.org/10.1016/j.fuel.2020.118963>.

[54] Duan P, Savage PE. Catalytic treatment of crude algal bio-oil in supercritical water: Optimization studies. *Energy. Environ Sci* 2011;4:1447–56. <https://doi.org/10.1039/c0ee00343c>.

[55] Frank ED, Elgowainy A, Han J, Wang Z. Life cycle comparison of hydrothermal liquefaction and lipid extraction pathways to renewable diesel from algae. *Mitig Adapt Strateg Glob Chang* 2013;18:137–58. <https://doi.org/10.1007/s11027-012-9395-1>.

[56] Ramirez JA, Brown RJ, Rainey TJ. A review of hydrothermal liquefaction bio-crude properties and prospects for upgrading to transportation fuels. *Energies (Basel)* 2015;8:6765–94. <https://doi.org/10.3390/en8076765>.

[57] P. Grange, E. Laurent, R. Maggi, A. Centeno, B. Delmon, Hydrotreatment of pyrolysis oils from biomass: reactivity of the various categories of oxygenated compounds and preliminary techno-economic study, 1996.

[58] Venderbosch RH, Ardyanti AR, Wildschut J, Oasmaa A, Heeres HJ. Stabilization of biomass-derived pyrolysis oils. *J Chem Technol Biotechnol* 2010;85:674–86. <https://doi.org/10.1002/jctb.2354>.

[59] Christensen E, McCormick RL. Long-term storage stability of biodiesel and biodiesel blends. *Fuel Process Technol* 2014;128:339–48. <https://doi.org/10.1016/j.fuproc.2014.07.045>.

[60] Araújo SV, Luna FMT, Rola EM, Azevedo DCS, Cavalcante CL. A rapid method for evaluation of the oxidation stability of castor oil FAME: influence of antioxidant type and concentration. *Fuel Process Technol* 2009;90:1272–7. <https://doi.org/10.1016/j.fuproc.2009.06.009>.

[61] Chen X, Ma X, Chen L, Lu X, Tian Y. Hydrothermal liquefaction of Chlorella pyrenoidosa and effect of emulsification on upgrading the bio-oil. *Biore sour Technol* 2020;316. <https://doi.org/10.1016/j.biortech.2020.123914>.

[62] Bouaid A, Martinez M, Aracil J. Long storage stability of biodiesel from vegetable and used frying oils. *Fuel* 2007;86:2596–602. <https://doi.org/10.1016/j.fuel.2007.02.014>.

[63] Z. Yaakob B.N. Narayanan S. Padikkaparambil S. Unni K., M. Akbar P., A review on the oxidation stability of biodiesel *Renewable and Sustainable Energy Reviews* 35 2014 136 153 10.1016/j.rser.2014.03.055.

[64] Flitsch S, Neu PM, Schober S, Kienzl N, Ullmann J, Mittelbach M. Quantitation of aging products formed in biodiesel during the Rancimat accelerated oxidation test. *Energy Fuel* 2014;28:5849–56. <https://doi.org/10.1021/ef501118r>.

[65] Türk J, Schmitt F, Anthofel T, Türk R, Ruck W, Krahl J. Extension of biodiesel aging mechanism—the role and influence of methyl oleate and the contribution of alcohols through the use of solketal. *ChemSusChem* 2023;16. <https://doi.org/10.1002/cssc.202300263>.

[66] Nguyen Lyckeskog H, Mattsson C, Åmand LE, Olausson L, Andersson SI, Vamling L, et al. Storage stability of bio-oils derived from the catalytic conversion of softwood kraft lignin in subcritical water. *Energy Fuel* 2016;30:3097–106. <https://doi.org/10.1021/acs.energyfuels.6b00087>.

[67] Wang Y, Zhang Y, Yoshikawa K, Li H, Liu Z. Effect of biomass origins and composition on stability of hydrothermal biocrude oil. *Fuel* 2021;302. <https://doi.org/10.1016/j.fuel.2021.121138>.

[68] Leng L, Yuan X, Chen X, Huang H, Wang H, Li H, et al. Characterization of liquefaction bio-oil from sewage sludge and its solubilization in diesel microemulsion. *Energy* 2015;82:218–28. <https://doi.org/10.1016/j.energy.2015.01.032>.